Environ Sci Pollut Res (2012) 19:2734–2744
DOI 10.1007/s11356-012-0773-8

RESEARCH ARTICLE

# Optimization of electrocoagulation process for the simultaneous removal of mercury, lead, and nickel from contaminated water

**Subramanyan Vasudevan · Jothinathan Lakshmi · Ganapathi Sozhan**

Received: 28 December 2011 / Accepted: 16 January 2012 / Published online: 4 February 2012
© Springer-Verlag 2012

**Abstract**
*Purpose and aim* The present study provides an optimization of electrocoagulation process for the simultaneous removal of heavy metals such as mercury, lead, and nickel from water. In doing so, the thermodynamic, adsorption isotherm and kinetic studies were also carried out.
*Materials and methods* Magnesium alloy, magnesium, aluminum, and mild steel sheet of size 2 $dm^2$ were used as anode and galvanized iron as cathode. To optimize the maximum removal efficiency, different parameters like effect of initial concentration, effect of temperature, pH, and effect of current density were studied. Mercury-, lead-, and nickel-adsorbed magnesium hydroxide coagulant was characterized by SEM and EDAX.
*Results* The results showed that the maximum removal efficiency was achieved for mercury, lead, and nickel with magnesium alloy as anode and galvanized iron as cathode at a current density of 0.15 Å/$dm^2$ and pH of 7.0. The adsorption of mercury, lead, and nickel are preferably fitting the Langmuir adsorption isotherm suggests monolayer coverage of adsorbed molecules. The adsorption process follows second-order kinetics. Temperature studies showed that adsorption was endothermic and spontaneous in nature.
*Conclusions* The magnesium hydroxide generated in the cell removes the heavy metals present in the water and reduces to a permissible level, making it drinkable.

**Keywords** Electrocoagulation · Heavy metal · Adsorption · Kinetics · Thermodynamics

Responsible editor: Vinod Kumar Gupta

S. Vasudevan (✉) · J. Lakshmi · G. Sozhan
CSIR—Central Electrochemical Research Institute,
Karaikudi 630 006, India
e-mail: vasudevan65@gmail.com

## 1 Introduction

It is well known that heavy metals constitute a serious threat for the environment and human health because they are not biodegradable. These heavy metals, known as powerful toxic agents, are teratogenic and carcinogenic (Collado-Sanchez et al. 1996; Carrington et al. 2004; Zhu and Alexandratos 2006; Kurniawan et al. 2006). Mercury, lead, and nickel are the most toxic non-essential heavy metals present in the environment. Elevated level of mercury, lead, and nickel ions arise from a variety of sources, such as batteries, accumulators made up of mercury (II) oxide, paints containing mercury (II) sulfate, pharmaceutical products like mercurochrome (antiseptic) and clinical thermometers, plating industries (Zhu and Alexandratos 2006). Mercury poisoning can affect the nervous system and cause neurological and renal disorders which are sometimes irreversible. Lead can cause central nervous system damage. Lead can also damage the kidney, liver and reproductive system, basic cellular processes, and brain functions. The toxic symptoms are anemia, insomnia, headache, dizziness, irritability, weakness of muscles, hallucination and renal damages. Nickel exceeding its critical level might bring about serious lung and kidney problems aside from gastrointestinal distress, pulmonary fibrosis and skin dermatitis. And it is known that nickel is human carcinogen (Carrington et al. 2004; Ullruich et al. 2001; Fitzgerald and Lamborg 2004). The drinking water guideline value for mercury, lead, and nickel recommended by World Health Organization (WHO) are 0.001, 0.025, and 0.020 mg/L, respectively (WHO 1993).

Conventional methods for removing heavy metals and its derivatives from water include ion exchange, reverse osmosis, co-precipitation, coagulation, complexation, solvent extraction, and adsorption. Physical methods like ion exchange, reverse osmosis and electrodialysis have proven to be either

too expensive or inefficient to remove mercury, lead, and nickel from water. At present, chemical treatments are not used due to disadvantages like high costs of maintenance, problems of sludge handling and its disposal, and neutralization of the effluent. The mercury, lead, and nickel removal from water by adsorption using different materials has also been explored. The major disadvantages of this studied adsorbent are low efficiency and high cost (Chen 2004; Alinsafi et al. 2005; Casqueira et al. 2006; Mercier and Pinnavaia 1998; Walcarius et al. 2003; Tonle et al. 2004; Tchinda et al. 2006).

Recent research has demonstrated that electrocoagulation offers an attractive alternative to above-mentioned traditional methods for treating water. In this process, anodic dissolution of metal electrode takes place with the evolution of hydrogen gas at the cathode. Electrochemically generated metallic ions from the anode can undergo hydrolysis to produce a series of activated intermediates that are able to adsorb (Gupta et al. 2006a, b; Gupta et al. 1997a, b; Gupta et al. 2003a, b; Gupta and Rastogi 2008a, b; Gupta and Rastogi 2009; Gupta et al. 2007a, b; Gupta et al. 1998; Gupta 1998; Gupta et al. 1999; Gupta and Ali 2000; Gupta et al. 2001; Gupta and Sharma 2002; Gupta and Sharma 2003; Mittal et al. 2010; Mohan et al. 2001; Srivastava et al. 1996; Srivastava et al. 1997) the contaminant present in the water to be treated alternatively or otherwise destabilize the finely dispersed particles present in the water. The advantages of electrocoagulation include high particulate removal efficiency, compact treatment facility, and possibility of complete automation (Vasudevan et al. 2008; Vasudevan et al. 2009; Vasudevan et al. 2010; Vasudevan and Lakshmi 2011). A literature survey shows that, in most of the studies, aluminum is used as anode material for the removal of contaminants from water using electrocoagulation. The main disadvantage in case of aluminum electrode is the residual aluminum (the USEPA guidelines suggest maximum contamination is 0.05–0.2 mg/L) present in the treated water due to cathodic dissolution. This will create health problems like cancer. In the case of magnesium electrodes, there is no such disadvantage like aluminum electrodes. Because the USEPA guidelines suggest maximum guidelines value of magnesium in water is 30 mg/L. Apart from the above, a literature survey does not show any study on the decontamination of mercury, lead, and nickel or its derivatives by electrocoagulation.

This article presents the results of the studies undertaken on the electrochemical removal of mercury, lead, and nickel using magnesium alloy, magnesium, aluminum, and mild steel as anodes and galvanized iron as cathode. To optimize the maximum removal efficiency of mercury, lead, and nickel, different parameters like effect of anode materials, initial mercury, lead, and nickel concentration, temperature, pH and current density were studied. The equilibrium adsorption behavior is analyzed by fitting models of Langmuir and Freundlich isotherms. Adsorption kinetics of electro coagulants is analyzed using first- and second-order kinetic models. Activation energy was evaluated to study the nature of adsorption.

## 2 Materials and methods

### 2.1 Experimental apparatus and procedures

The electrolytic cell (Fig. 1) consisted of a 1.0-L Plexiglas vessel that was fitted with a poly(vinyl chloride) cell cover with slots to introduce the electrodes, pH sensor, a thermometer and the electrolytes. Magnesium alloy (Magnesium Elektron Ltd; AZ31 consisting of 3.0 wt.% Al and 1.0 wt.% Zn), magnesium (commercial grade, India), aluminum (commercial grade, India), and mild steel (commercial grade, India) of surface area (0.02 $m^2$) acted as the anode. The cathodes were galvanized iron (commercial grade) sheets of the same size as the anode. The temperature of the electrolyte was controlled to the desired value with a variation of ±2 K by adjusting the rate of flow of thermostatically controlled water through an external glass-cooling spiral. A regulated direct current was supplied from a rectifier (10 Å, 0–25 V; Aplab model).

Mercury as $Hg(NO_3)_2$, lead as $Pb(NO_3)_2$, and nickel as $Ni(NO_3)_2$ (Merck, Germany; Analar Reagent) was dissolved in drinking water for the required concentration (0.1–0.5 mg/L). 0.90 L of solution was used for each experiment, which was used as the electrolyte. The pH of the electrolyte was adjusted, if required, with HCl or NaOH solutions before experiments.

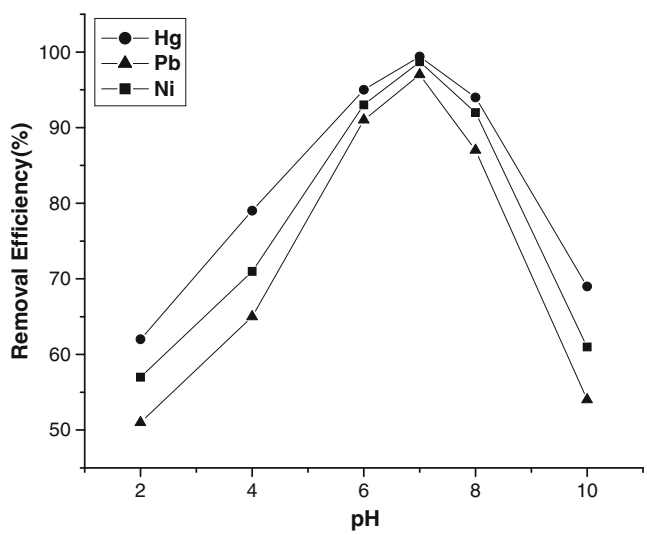


**Fig. 1** Effect of pH of the electrolyte on the removal of mercury, nickel, and lead conditions, concentration of mercury, lead, and nickel, 0.1 mg/l; solution temperature, 305 K; anode, magnesium alloy; cathode, galvanized iron; current density, 0.15 Å$dm^{-2}$; duration, 30 min

### 2.2 Analytical procedure

The analysis of mercury, lead, nickel, magnesium, aluminum, and zinc were characterized UV–Visible spectrophotometer (MERCK, Pharo 300). The scanning electron microscopy (SEM) and energy-dispersive X-ray spectroscopy (EDAX) images of magnesium hydroxide were analyzed with a SEM made by Hitachi (model s-3000h). The Fourier transform infrared spectrum of magnesium hydroxide was obtained using Nexus 670 FTIR spectrometer made by Thermo Electron Corporation, USA.

## 3 Theory

### 3.1 Kinetic modeling

The magnesium hydroxide complexes formed during electrocoagulation remain in the aqueous stream as metal hydroxides. These metal hydroxides, charged hydroxyl-cationic complexes, can effectively remove pollutants by adsorption and produce charge neutralization by complexation, electrostatic attraction, and enmeshment in a precipitate. The electrode consumption can be estimated according to Faraday's law, and the amount of generated metal hydroxides can be stoichiometrically determined. Since the amount of coagulant can be estimated for a given time, the pollutant removal can be modeled using an adsorption phenomenon (Veli and Ozturk 2005). In order to investigate the mechanisms of the mercury, lead, and nickel adsorption process, two different kinetic models (Gupta et al. 2003a, b), the pseudo-first-order model and pseudo-second-order model, were applied to describe the kinetics of the mercury, lead, and nickel adsorption onto magnesium hydroxides.

#### *3.1.1 First-order Lagergren model*

The first-order rate equation of the Lagergren model is one of the most widely used expressions describing the adsorption of solute from a solution. The first-order Lagergren model is generally expressed as follows (Sharma and Bhattacharyya 2004),

$$\mathrm{d}q_t/\mathrm{d}t = k_1(q_\mathrm{e} - q_t) \tag{1}$$

where $q_\mathrm{e}$ and $q_t$ are the adsorption capacities at equilibrium and at time $t$ (min) respectively, and $k_1$ ($\mathrm{min}^{-1}$) is a rate constant of first-order adsorption. The integrated form of the above equation with the boundary conditions $t$=0 to >0 ($q$=0 to >0) is rearranged to obtain the following time dependence function,

$$\log(q_\mathrm{e} - q_t) = \log(q_\mathrm{e}) - k_1 t/2.303 \tag{2}$$

#### *3.1.2 Second-order Lagergren model*

The Lagergren second-order kinetic model is expressed as (Ho and McKay 1998),

$$\mathrm{d}q_t/\mathrm{d}t = k_2(q_\mathrm{e} - q_t)^2 \tag{3}$$

where $k_2$ is the rate constant of second-order adsorption. The integrated form of Eq. 3 with the boundary condition $t$=0 to >0 ($q$=0 to >0) is,

$$1/(q_\mathrm{e} - q_t) = 1/q_\mathrm{e} + k_2 t \tag{4}$$

Equation 4 can be rearranged and linearized as,

$$t/q_t = 1/k_2 {q_\mathrm{e}}^2 + t/q_\mathrm{e} \tag{5}$$

where, $q_\mathrm{e}$ and $q_t$ are the amount of mercury, lead, and nickel adsorbed on $Mg(OH)_2$ (mg $g^{-1}$) at equilibrium and at time $t$ (min), respectively, and $k_2$ is the rate constant for the second-order kinetic model.

### 3.2 Isotherm modeling

The pollutant is generally adsorbed at the surface of the metal hydroxides generated during the electrocoagulation process. Thus, the removal of pollutant is similar to conventional adsorption, except for coagulants generated. Coagulated particles attract and absorb different ions and colloidal particles from the water. In order to identify the mechanism of the adsorption process, it is important to establish the most appropriate correlation for the equilibrium curves. In this study, two adsorption isotherms, Langmuir and Freundlich, were applied to establish the relationship between the amounts of mercury, lead, and nickel adsorbed onto the magnesium hydroxides and its equilibrium concentration in the aqueous solution containing mercury, lead, and nickel.

#### *3.2.1 Freundlich isotherm*

The Freundlich adsorption isotherm typically fits the experimental data over a wide range of concentrations. This empirical model includes considerations of surface heterogeneity and exponential distribution of the active sites and their energies. The isotherm is adopted to describe reversible adsorption and is not restricted to monolayer formation. The linearized in logarithmic form and the Freundlich constants can be expressed as (Freundlich 1907),

$$\log q_\mathrm{e} = \log k_\mathrm{f} + n \log C_\mathrm{e} \tag{6}$$

where, $k_\mathrm{f}$ is the Freundlich constant related to adsorption capacity, $n$ is the energy or intensity of adsorption, $C_\mathrm{e}$ is the equilibrium concentration of mercury, lead, and nickel (mg $L^{-1}$).

*3.2.2 Langmuir isotherm*

The Langmuir model was originally developed to represent chemisorption at a set of well-defined localized adsorption sites with the same adsorption energy, independent of the surface coverage, and with no interaction between adsorbed molecules. This model assumes a monolayer deposition on a surface with a finite number of identical sites (Mckay et al. 1982). It is well known that the Langmuir equation is valid for a homogeneous surface. The linearized form of Langmuir adsorption isotherm model is,

$$C_e/q_e = 1/q_m b + C_e/q_m \quad (7)$$

where, $q_e$ is amount adsorbed at equilibrium concentration $C_e$, $q_m$ is the Langmuir constant representing maximum monolayer adsorption capacity and $b$ is the Langmuir constant related to energy of adsorption. The essential characteristics of the Langmuir isotherm can be expressed as the dimensionless constant $R_L$.

$$R_L = 1/(1 + bC_o) \quad (8)$$

where $R_L$ is the equilibrium constant it indicates the type of adsorption, $b$, is the Langmuir constant (Langmuir 1918). $C_o$ is various concentrations of mercury, lead, and nickel solution. The $R_L$ values between 0 and 1 indicate the favorable adsorption.

### 3.3 Thermodynamic parameters

To understand the effect of temperature on the adsorption process, thermodynamic parameters should be determined at various temperatures (Golder et al. 2006). The energy of activation for adsorption of mercury, lead, and nickel can be determined by the second-order rate constant is expressed in Arrhenius form.

$$\ln k_2 = \ln k_o - E/RT \quad (9)$$

where $k_o$ is the constant of the equation (g mg$^{-1}$ min$^{-1}$), $E$ is the energy of activation (J mol$^{-1}$), $R$ is the gas constant (8.314 Jmol$^{-1}$ K$^{-1}$), and $T$ is the temperature in K. The free energy change is obtained using the following relationship

$$\Delta G = -RT \ln K_c \quad (10)$$

where $\Delta G$ is the free energy (kJ mol$^{-1}$), $K_c$ is the equilibrium constant, $R$ is the gas constant and $T$ is the temperature in $K$. Other thermodynamic parameters such as entropy change ($\Delta S$) and enthalpy change ($\Delta H$) were determined using van't Hoff equation,

$$\ln K_c = \frac{\Delta S}{R} - \frac{\Delta H}{RT} \quad (11)$$

Enhancement of adsorption capacity of electrocoagulant (magnesium hydroxide) at higher temperatures may be attributed to the enlargement of pore size and or activation of the adsorbent surface.

## 4 Results and discussion

### 4.1 Effect of anode materials

It is well known that water treatment with coagulants such as aluminum alum, ferric chloridem and ferric sulfate are effective in removing mercury, lead, and nickel from drinking water. Contaminants present in the water will be removed by the adsorption with metal hydroxides produced from the respective coagulants. The main disadvantage for the above process is the presence of anions like chloride and sulfate will reduce the removal efficiency and will increase the total dissolved solids in the treated water. So to overcome the above difficulties, in the present investigation, magnesium alloy, magnesium, aluminum, and mild steel are used as anode (in situ generation of the coagulants) and galvanized iron is used as cathode material. The electrochemical ion generation has several distinct advantages. Coagulants introduced without corresponding sulfate or chloride ions are more efficient at removing contaminants from water. By eliminating competing anions and using a highly pure coagulant source, lower metals residuals are obtained and less sludge is produced than when metal salts are utilized. A contaminant-free ion source allows maximum adsorptive removal of the various dissolved forms of metals that could be present and require treatment. Contaminants present in industrial-grade ferrous sulfate and aluminum salts end up in either the treated effluent or sludge cake. If flow rates or contaminant loads fluctuate, chemical treatment systems are difficult to operate but it is not in the case of electrochemical process.

During the electrolysis of magnesium alloy, (or) magnesium, (or) aluminum, (or) iron, hydroxides of micro-flocs are formed rapidly by anodic dissolution. After the electrolysis process, the water is gently stirred for few minutes for agglomeration of micro-flocs into larger easily settleable flocs. During this flocculation process, all kinds of micro particles and charged ions are attached to the flocs by electrostatic attachment. Mercury, lead, and nickel is also adsorbed onto coagulated flocs. The possible reactions of magnesium alloy, aluminum, and mild steel for the formation of hydroxides are as follows:

At the cathode,

$$2H_2O + 2e^- \rightarrow H_2(g) + 2OH^- \quad (12)$$

At the anode, (when magnesium alloy/magnesium as anode):

$$Mg \rightarrow Mg^{2+} + 2e^- \quad (13)$$

$$Mg^{2+}(aq) + 2H_2O \rightarrow Mg(OH)_2 + 2H^+(aq) \quad (14)$$

(when aluminum as anode)

$$Al \rightarrow Al^{3+} + 3e^- \quad (15)$$

$$Al^{3+}(aq) + 3H_2O \rightarrow Al(OH)_3 + 3H^+(aq) \quad (16)$$

(when iron as anode)

$$4Fe(s) \rightarrow 4Fe^{2+}(aq) + 8e^- \quad (17)$$

$$4Fe(s) + 10H_2O(l) + O_2(g) \rightarrow Fe(OH)_3(s) + 4H_2(g) \quad (18)$$

Mercury, lead, and nickel adsorbed on hydroxide flocs and removed by filtration. From Table 1, it is concluded that the magnesium alloy electrode is more effective in removing mercury, lead, and nickel than mild steel and the removal efficiency is very close to using an aluminum electrode. Apart from the lower removal efficiency of aluminum electrode, the main disadvantage in case of aluminum electrode is the residual aluminum (The USEPA guidelines suggest maximum contamination is 0.05–0.2 mg/L) present in the treated water due to cathodic dissolution. This will create health problems like cancer. In the case of mild steel electrode, the maximum contamination limit is 0.2 mg/L (USEPA guidelines). In the case of magnesium electrodes, there is no such disadvantage like aluminum and mild steel electrodes. Because the USEPA guidelines suggest maximum guidelines value of magnesium in water is 30 mg/L. To evaluate the alternative anodes material for mercury, lead, and nickel removal from water, further studies were carried out with magnesium alloy as anode material.

### 4.2 Effect of pH

It is believed that the initial pH is an important operating factor influencing the performance of electrochemical process. To explain this effect, a series of experiments were carried out using 0.1 mg/L mercury, lead, and nickel containing solutions, by adjusting the initial pH in the interval from 2 to 10. The removal efficiency of mercury, lead, and nickel was increased with increasing the pH up to 7 (Fig. 1). When the pH is above 7, removal efficiency should be decreased. The decrease of removal efficiency at more acidic and alkaline pH was observed by many investigators (Vasudevan et al. 2009) and was attributed to an amphoteric behavior of $Al(OH)_3$ which leads to soluble $Al^{3+}$ cations (at acidic pH) and to monomeric anions $Al(OH)^{4-}$ (at alkaline pH). It is well known that these soluble species are not useful for water treatment. When the initial pH was kept in neutral, all the aluminum produced at the anode formed polymeric species ($Al_{13}O_4(OH)_{24}{}^{7+}$) and precipitated $Al(OH)_3$ leading to more removal efficiency (Vasudevan et al. 2009). In the present study, the electrolyte pH was maintained in neutral, so the formation of $Mg(OH)_2$ is more predominant (like aluminum), leading to greater removal efficiency.

### 4.3 Effect of inter-electrode distance

To determine the effect various inter-electrode distances between anode and cathode, the electrodes were kept at different spacing viz., 0.003, 0.005, 0.007, 0.009, and 0.011 m. The experiments were conducted with 0.1 mg/L mercury, lead, and nickel each containing solutions at a current density of 0.15 Å$dm^{-2}$. The results of inter-electrode distance on removal efficiency and energy consumption are presented in Fig. 2. While decreasing the inter-electrode distance shows decrease in energy consumption and increase in removal efficiency. Short distance between each electrode requires lesser electrical energy for motion of ions due to shorter travel path that reduce the resistance of motion and the situation is reverse for the case of large distance between each electrode. But in maintaining the inter-electrode distance of 0.003 m was practically difficult. So, the further experiments were carried out at inter-electrode distance of 0.005 m. Inter-electrode spacing of 0.005 m had the low energy consumption and removal efficiency.

**Table 1** Effect of different anodes for the removal of mercury, lead, and nickel at 0.1 mg/L each. Current density—0.15 Å/$dm^2$

| Anode material | Voltage (V) | Final concentration (mg/L) | | | Removal efficiency (%) | | |
|---|---|---|---|---|---|---|---|
| | | Mercury | Lead | Nickel | Mercury | Lead | Nickel |
| Magnesium alloy | 1.5 | 0.001 | 0.002 | 0.001 | 99 | 98 | 99 |
| Magnesium | 2.1 | 0.011 | 0.009 | 0.007 | 89 | 91 | 93 |
| Aluminum | 2.2 | 0.023 | 0.015 | 0.014 | 77 | 85 | 86 |
| Mild steel | 2.1 | 0.062 | 0.046 | 0.042 | 38 | 54 | 58 |

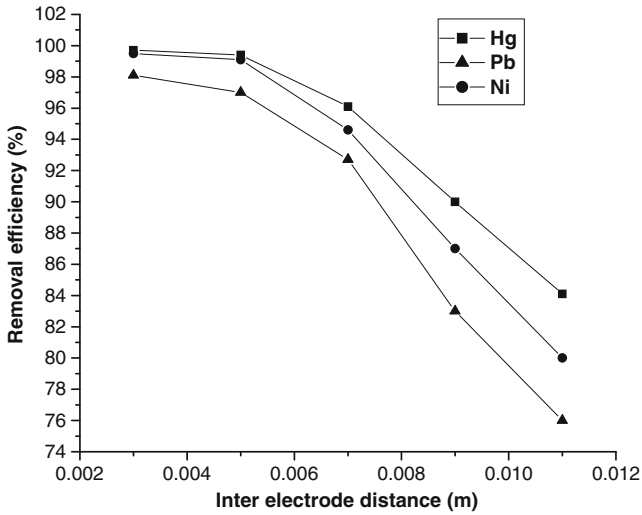


**Fig. 2** Effect of inter-electrode distance on the removal of mercury, lead, and nickel. Conditions, solution pH, 7.0; solution temperature, 305 K; anode, magnesium alloy; cathode, galvanized iron; current density, 0.15 Å/dm$^2$; duration, 30 min

## 4.4 Effect of current density

Operating current density is critical in electrocoagulation, as it is the only operational parameter that can be controlled directly. Current density directly determines both coagulant dosage and bubble generation rates, as well as strongly influencing both solution mixing and mass transfer at the electrodes. Thus, a set of experiments were carried out to quantify the impact of operating current on reactor performance. A serious of experiments were carried out using 0.1 mg/L of mercury, lead, and nickel containing electrolyte, at pH 7.0, with the current density being varied from 0.025 to 0.2 Å dm$^{-2}$. The plot shows that the uptake of mercury, lead, and nickel (in milligrams per gram) increased with increase in current density and remained nearly constant after equilibrium time (figure not shown). The equilibrium time was found to be 30 min for all concentration studied. After 30 min, the amount of mercury, lead, and nickel adsorbed ($q_e$) increased from 0.0744 to 0.0983 mg/g as the current density increased from 0.025–0.2 mg/L. The plots are single, smooth and continuous curves leading to saturation, suggesting the possible monolayer coverage to mercury, lead, and nickel on the surface of the adsorbent. Further, the amount of heavy metal in water removal depends upon the quantity of adsorbent (magnesium hydroxide) generated, which is related to the time and current density.

## 4.5 Kinetic modeling

In the present investigation, two kinetic models, namely, the first- and second-order models were tested with the mercury, lead, and nickel concentration of 0.1 mg/L at various current densities from 0.025–0.2 Å/dm$^2$.

### *4.5.1 First-order Lagergren model*

The experimental data were analyzed initially with first-order Lagergren model. The plot of log ($q_e - q_t$) vs $t$ should give the linear relationship from which $k_1$ and $q_e$ can be determined by the slope and intercept, respectively (Eq. 2). The computed results are presented in Table 2. The results show that the theoretical $q_e$(cal) value does not agree to the experimental $q_e$ (exp) values at all concentrations studied with poor correlation coefficient. So, further, the experimental data were fitted with second-order Lagergren model.

### *4.5.2 Second-order Lagergren model*

The kinetic data were fitted to the second-order Lagergren model (Eq. 5). The equilibrium adsorption capacity, $q_e$(cal) and $k_2$ were determined from the slope and intercept of plot of $t/q_t$ versus $t$ and are compiled in Table 2. Figure 3 shows the plot of $t/q_t$ versus $t$ for mercury adsorption. The plots were found to be linear with good correlation coefficients. The theoretical $q_e$(cal) values agree well to the experimental $q_e$(exp) values at all current density studied. This implies that the second-order model is in good agreement with experimental data and can be used to favorably explain the mercury, lead, and nickel adsorption on $Mg(OH)_2$.

Table 2 depicts the computed results obtained from first- and second-order models. From the tables, it is found that second-order shows good correlation coefficient than first-order model. Further, the calculated $q_e$ values well agrees with the experimental $q_e$ values for second-order kinetics model concluding that the second-order kinetics equation is the best-fitting kinetic model.

## 4.6 Isotherm modeling

### *4.6.1 Freundlich isotherm*

In testing the isotherm, the mercury, lead, and nickel concentration used was 0.1–0.5 mg/L with various current density from 0.025–0.2 Å/dm$^2$ and at an initial pH of 7. The adsorption data is plotted as log $q_e$ versus log $C_e$ by Eq. 6 should result in a straight line with slope $n$ and intercept $k_f$. The intercept and the slope are indicators of adsorption capacity and adsorption intensity, respectively. Values of $n$ falling in the range of 1–10 indicate favorable sorption. $k_f$ and $n$ values were listed in Table 3 for each concentration and current density. It has been reported that values of $n$ lying between 0 and 10 indicate favorable adsorption. From the analysis of the results it is found that the Freundlich plots fit satisfactorily with the experimental data obtained in the present study.

**Table 2** Comparison between the experimental and calculated $q_e$ values at different current density in first- and second-order adsorption kinetics with concentration 0.1 mg/L at room temperature

| Contaminant | Current density (Å/dm$^2$) | $q_e$ (exp) | First-order adsorption | | | Second-order adsorption | | |
|---|---|---|---|---|---|---|---|---|
| | | | $q_e$(cal) | $k_1 \times 10^4$ (min/mg) | $R^2$ | $q_e$(cal) | $k_2 \times 10^4$ (min/mg) | $R^2$ |
| Mercury | 0.025 | 0.0062 | 8.77 | −0.0033 | 0.7655 | 0.0064 | 0.0835 | 0.9998 |
| | 0.05 | 0.0071 | 9.99 | −0.0051 | 0.7881 | 0.0069 | 0.0915 | 0.9964 |
| | 0.1 | 0.0072 | 10.87 | −0.0058 | 0.8135 | 0.0070 | 0.0917 | 0.9991 |
| | 0.15 | 0.0073 | 11.64 | −0.0066 | 0.7864 | 0.0071 | 0.0919 | 0.9996 |
| | 0.2 | 0.0075 | 12.87 | −0.0070 | 0.7866 | 0.0072 | 0.0965 | 0.9957 |
| Lead | 0.025 | 0.0631 | 9.94 | −0.0039 | 0.7854 | 0.0628 | 0.0831 | 0.9999 |
| | 0.05 | 0.0714 | 10.49 | −0.0048 | 0.7967 | 0.0701 | 0.0906 | 0.9998 |
| | 0.1 | 0.0733 | 10.55 | −0.0055 | 0.8005 | 0.0715 | 0.0912 | 0.9989 |
| | 0.15 | 0.0756 | 10.61 | −0.0060 | 0.7457 | 0.0744 | 0.0919 | 0.9964 |
| | 0.2 | 0.0799 | 10.97 | −0.0061 | 0.7598 | 0.0745 | 0.0933 | 0.9945 |
| Nickel | 0.025 | 0.0665 | 12.31 | −0.0044 | 0.7655 | 0.0654 | 0.0822 | 0.9999 |
| | 0.05 | 0.0771 | 12.64 | −0.0053 | 0.7881 | 0.0745 | 0.0897 | 0.9997 |
| | 0.1 | 0.0784 | 12.99 | −0.0058 | 0.8135 | 0.0781 | 0.0901 | 0.9996 |
| | 0.15 | 0.0866 | 13.65 | −0.0061 | 0.7864 | 0.0854 | 0.0917 | 0.9983 |
| | 0.2 | 0.0891 | 13.97 | −0.0064 | 0.7866 | 0.0894 | 0.0999 | 0.9981 |

### *4.6.2 Langmuir isotherm*

Langmuir isotherm was tested from Eq. 7. The plots of $1/q_e$ as a function of $1/C_e$ for the adsorption of mercury, lead, and nickel on $Mg(OH)_2$ are shown in Fig. 4. The plots were found linear with good correlation coefficients (>0.99) indicating the applicability of Langmuir model in the present study. The values of monolayer capacity ($q_m$) and Langmuir constant ($b$) is given in Table 3. The values of $q_m$ calculated by the Langmuir isotherm were all close to experimental values at given experimental conditions. These facts suggest that mercury, lead, and nickel are adsorbed in the form of monolayer coverage on the surface of the adsorbent. The sorption isotherms of mercury, lead, and nickel on magnesium hydroxide typically follow Langmuirian behavior as described by previous researchers.

The dimensionless constant $R_L$ were calculated from Eq. 8. The $R_L$ values were found to be between 0 and 1 for all the concentration of mercury, lead, and nickel studied.

The correlation coefficient values of Langmuir and Freundlich isotherm models are presented in Table 3. The Langmuir isotherm model has higher regression coefficient ($R^2$=0.999) when compared to the other models indicating the Langmuir model provide a better description of the process.

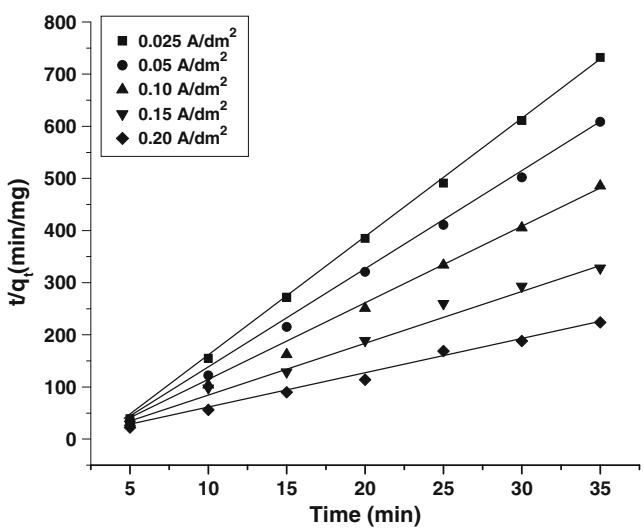


**Fig. 3** Second-order kinetic model plots for adsorption of mercury at different current densities. Conditions—concentration, 2 mg/L; temperature, 305 K; pH of the electrolyte, 7.0

**Table 3** Constant parameters and correlation coefficient for different adsorption isotherm models for mercury, lead, and nickel adsorption at 0.1–0.5 mg/L at a current density of 0.15 Å/dm$^2$

| Isotherm | Parameters | Contaminants | | |
|---|---|---|---|---|
| | | Mercury | Lead | Nickel |
| Langmuir | $q_m$ (mg/g) | 1.8471 | 2.1129 | 2.4554 |
| | $b$(L/mg) | 4.8321 | 4.9864 | 5.2565 |
| | $R^2$ | 0.9989 | 0.9994 | 0.9997 |
| | $R_L$ | 0.5978 | 0.6424 | 0.5564 |
| Freundlich | $k_f$ (mg/g) | 1.6621 | 1.5959 | 1.5525 |
| | $n$ (L/mg) | 1.0363 | 1.0412 | 1.0861 |
| | $R^2$ | 0.9823 | 0.9856 | 0.9885 |

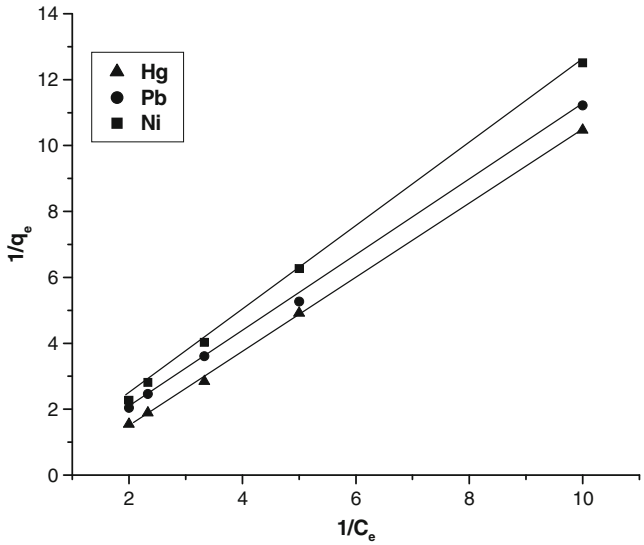


**Fig. 4** Langmuir plot ($1/q_e$ vs $1/C_e$) for adsorption of mercury, lead, and nickel. Conditions—pH of the electrolyte, 7.0; current density, 0.15 Å$dm^{-2}$; temperature, 303 K; and concentration, 0.1–0.5 mg/L

## 4.7 Thermodynamic parameters

Figure 5 shows that the rate constants vary with temperature according to Eq. 9 for mercury, lead, and nickel. The activation energy is calculated from slope of the fitted equation. The free energy change is obtained from Eq. 11. The $K_c$ and $\Delta G$ values are presented in Table 4. From the table, it is found that the negative value of $\Delta G$ indicates the spontaneous nature of adsorption. The enthalpy change and entropy change were obtained from the slope and intercept of the van't Hoff linear plots of $\ln K_c$ versus $1/T$ (Fig. 6; Eq. 11) for mercury, lead, and nickel. Positive value of enthalpy change ($\Delta H$) indicates that the adsorption process is endothermic in nature, and the negative value of change in internal energy ($\Delta G$) show the spontaneous adsorption of mercury, lead, and nickel on the adsorbent. Positive values of entropy change show the increased randomness of the solution interface during the adsorption of mercury, lead, and nickel on the adsorbent (Table 4). Enhancement of adsorption capacity of electro coagulant (magnesium hydroxide) at higher temperatures may be attributed to the enlargement of pore size and or activation of the adsorbent surface. Using Lagergren rate equation, second-order rate constants and correlation coefficient were calculated for different temperatures (305–343 K). The calculated '$q_e$' values obtained from the second-order kinetics agrees with the experimental '$q_e$' values better than the first-order kinetics model, indicating adsorption following second-order kinetics. Table 5 depicts the computed results obtained from first- and second-order kinetic models.

**Table 4** Thermodynamics parameters for adsorption of mercury, lead, and nickel

| Contaminant | Temp (K) | $K_c$ | $\Delta G°$ (J/mol) | $\Delta H°$ (kJ/mol) | $\Delta S°$ (J/mol/K) |
|---|---|---|---|---|---|
| Mercury | 323 | 11.21 | −192.31 | 3.6624 | 1.2665 |
| | 333 | 12.37 | −185.34 | | |
| | 343 | 13.09 | −159.64 | | |
| Lead | 323 | 12.33 | −201.65 | 3.4561 | 1.1165 |
| | 333 | 13.41 | −196.22 | | |
| | 343 | 13.99 | −180.23 | | |
| Nickel | 323 | 13.62 | −237.32 | 3.0064 | 0.9467 |
| | 333 | 14.31 | −215.36 | | |
| | 343 | 15.45 | −211.22 | | |

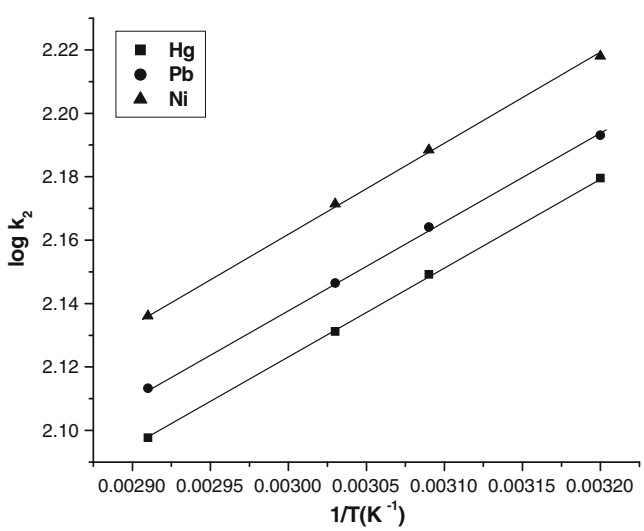


**Fig. 5** Plot of log $k_2$ and $1/T$. Conditions—pH of 7.0, current density, 0.15 Å/$dm^2$, and concentration, 0.1–0.5 mg/L

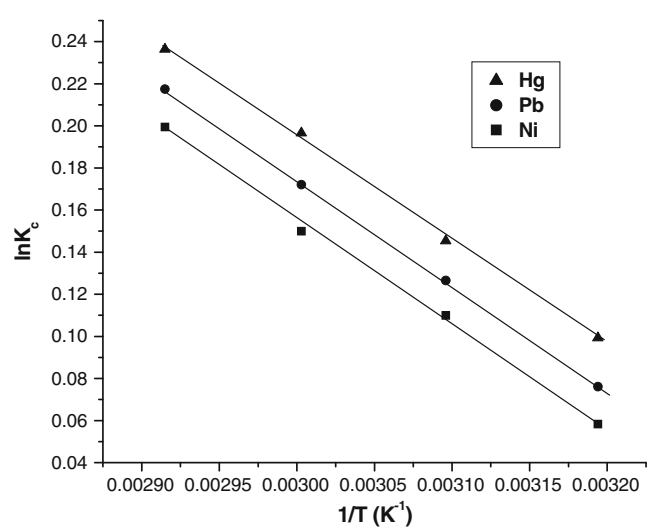


**Fig. 6** Plot of $\ln K_c$ and 1/T. Conditions—pH of the electrolyte, 7.0; current density, 0.15 Å/$dm^2$, and concentration, 0.1–0.5 mg/L

**Table 5** Comparison between the experimental and calculated $q_e$ values for the mercury, lead, and nickel concentration of 0.1 mg/L at 0.15 Å/dm$^2$ in first- and second-order adsorption kinetics

| Contaminant | Temp (K) | $q_e$ (exp) | First-order adsorption | | | Second-order adsorption | | |
|---|---|---|---|---|---|---|---|---|
| | | | $q_e$(cal) | $k_1 \times 10^4$ (min/mg) | $R^2$ | $q_e$(cal) | $k_2 \times 10^4$ (min/mg) | $R^2$ |
| Mercury | 323 | 0.0072 | 10.87 | −0.0054 | 0.8112 | 0.0070 | 0.0901 | 0.9998 |
| | 333 | 0.0071 | 11.64 | −0.0061 | 0.7866 | 0.0071 | 0.0908 | 0.9999 |
| | 343 | 0.0070 | 12.87 | −0.0063 | 0.7845 | 0.0072 | 0.0911 | 0.9994 |
| Lead | 323 | 0.0781 | 10.25 | −0.0059 | 0.8005 | 0.0715 | 0.0912 | 0.9989 |
| | 333 | 0.0786 | 10.37 | −0.0063 | 0.7457 | 0.0744 | 0.0919 | 0.9964 |
| | 343 | 0.0794 | 10.65 | −0.0065 | 0.7598 | 0.0745 | 0.0933 | 0.9945 |
| Nickel | 323 | 0.0786 | 13.01 | −0.0064 | 0.8011 | 0.0776 | 0.0971 | 0.9999 |
| | 333 | 0.0799 | 13.85 | −0.0067 | 0.7964 | 0.0763 | 0.0976 | 0.9988 |
| | 343 | 0.0804 | 14.15 | −0.0073 | 0.7869 | 0.0794 | 0.0979 | 0.9994 |

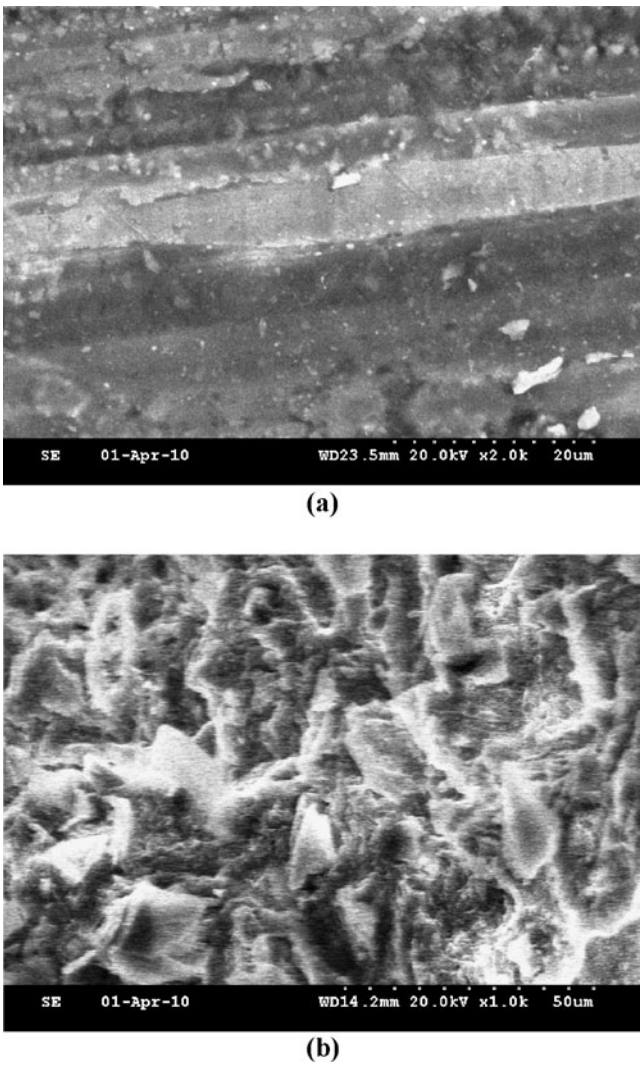


**Fig. 7** SEM image of the anode **a** before, **b** after treatment

## 4.8 Surface morphology

### *4.8.1 SEM and EDAX studies*

SEM images of magnesium anode, before and after, electrocoagulation of mercury electrolyte was obtained to compare the surface texture. Figure 7a shows the original magnesium alloy plate surface prior to its use in electrocoagulation experiments. The surface of the electrode is uniform. Figure 7b shows the SEM of the same electrode after several cycles of use in electrocoagulation experiments. The electrode surface is now found to be rough, with a number of dents. These dents are formed around the nucleus of the active sites where the electrode dissolution results in the production of magnesium hydroxides. The formation of a large number of dents may be attributed to the anode material consumption at active sites due to the generation of oxygen at its surface.

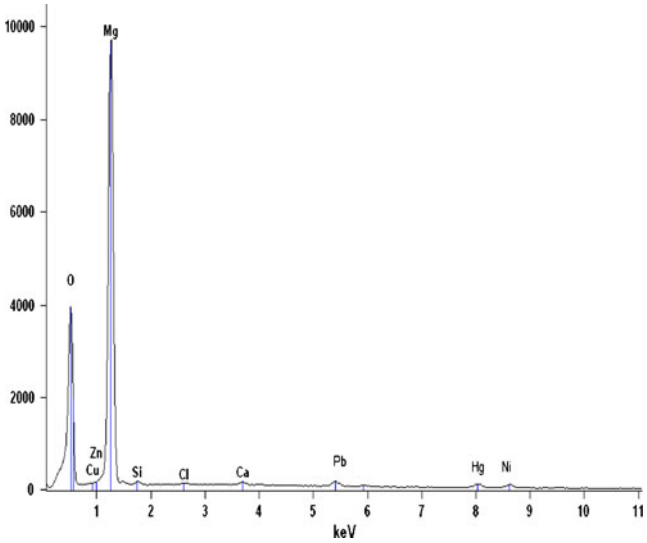


**Fig. 8** EDAX spectrum of mercury-, lead-, and nickel-adsorbed magnesium hydroxide

Energy-dispersive analysis of X-rays was used to analyze the elemental constituents of mercury-, lead-, and nickel-adsorbed magnesium hydroxide shown in Fig. 8. It shows that the presence of Hg, Pb and Ni, Mg and O appears in the spectrum. EDAX analysis provides direct evidence that mercury, lead, and nickel is adsorbed on magnesium hydroxide. Other elements detected in the adsorbed magnesium hydroxide come from adsorption of the conducting electrolyte, chemicals used in the experiments, alloying and the scrap impurities of the anode and cathode.

## 5 Conclusions

The results showed that the maximum removal efficiency was achieved at a current density of 0.15 Å/dm$^2$ and pH of 7.0 for mercury, lead, and nickel using magnesium alloy as anode and galvanized iron as cathode. The anodically dissolved magnesium hydroxide adsorbs on magnesium and removes the mercury, lead, and nickel below 0.05 mg/L. From the Lagergren model of kinetic studies, it is showed the adsorption is depends on both magnesium hydroxide and mercury, lead, and nickel concentrations that is second-order kinetics. The adsorption of mercury, lead, and nickel preferably fit for Langmuir adsorption isotherm rather than Freundlich isotherms. The temperature studies showed that the adsorption process is an endothermic and spontaneous process.

**Acknowledgment** The authors wish to express their gratitude to the Director, Central Electrochemical Research Institute, Karaikudi, for aid in publishing this article.

## References

Alinsafi A, Khemis M, Pons MN, Leclerc JP, Yaacoubi A, Benhammou A, Nejmeddine A (2005) Electrocoagulation of reactive textile dyes and textile wastewater. Chem Eng Proc 44:461–470

Carrington CD, Montwill B, Bolger PM (2004) An intervention analysis for reduction of exposure to methylmercury from the consumption of sea food by women of child-bearing age. Regul Toxicol Pharma 40:272–280

Casqueira RG, Toren ML, Kohler HM (2006) The removal of zinc from liquid streams by electroflotation. Miner Eng 19:1388–1392

Chen G (2004) Electrochemical technologies in wastewater treatment. Sep Purif Technol 38:11–41

Collado-Sanchez C, Pérez-Pena J, Gelado-Caballero MD, Herrera-Melian JA, Hernandez-Brito JJ (1996) Rapid determination of copper, lead and cadmium in unpurged seawater by adsorptive stripping voltammetry. Anal Chim Acta 320:19–30

Fitzgerald WF, Lamborg CH (2004) Geochemistry of mercury in the environment. In: Holland HD, Turckian KK (eds) Treatise on Geochemistry. Elsevier, Oxford, UK

Freundlich H (1907) Ueber die adsorption in Loesungen. Physic Chem 57:385–470

Golder AK, Samantha AN, Ray S (2006) Removal of phosphate from aqueous solution using calcined metal hydroxides sludge waste generated from electrocoagulation. Sep Purif Technol 52:102–109

Gupta VK (1998) Equilibrium uptake, sorption dynamics, process development and column operations for the removal of copper and nickel from aqueous solution and wastewater using activated slag—a low cost adsorbent. Ind Eng Chem Res 37:192–202

Gupta VK, Ali I (2000) Utilization of bagasse fly ash (a sugar industry waste) for the removal of copper and zinc from wastewater. Sep Purif Technol 18:131–140

Gupta VK, Rastogi A (2008a) Biosorption of lead from aqueous solutions by green algae Spirogyra species: Equilibrium and adsorption kinetics. J Hazard Mater 152:407–414

Gupta VK, Rastogi A (2008b) Equilibrium and kinetic modeling of cadmium (II) biosorption by nonliving algal biomass *Oedogonium* sp. from aqueous phase. J Hazar Mater 153:759–766

Gupta VK, Rastogi A (2009) Biosorption of hexavalent chromium by raw and acid-treated green alga Oedogonium hatei from aqueous solutions. J Hazard Mater 163:396–402

Gupta VK, Sharma S (2002) Removal of cadmium and zinc from aqueous solutions using red mud. Environ Sci Technol 36:3612–3617

Gupta VK, Sharma S (2003) Removal of zinc from aqueous solutions using bagasse fly ash—a low cost adsorbent. Ind Eng Chem Res 42:6619–6624

Gupta VK, Ali I, Saini VK (1997a) Adsorption studies on the removal of Vertigo Blue 49 and Orange DNA13 from aqueous solutions using carbon slurry developed from a waste material. J Colloid Interface Sci 315:87–93

Gupta VK, Rastogi A, Dwivedi MK, Mohan D (1997b) Process development for the removal of zinc and cadmium from wastewater using slag—a blast furnace waste material. Sep Sci Technol 32:2883–2912

Gupta VK, Srivastava SK, Mohan D, Sharma S (1998) Design parameters for fixed bed reactors of activated carbon developed from fertilizer waste material for the removal of some heavy metal ions. Waste Manage 17:517–522

Gupta VK, Mohan D, Sharma S, Park KT (1999) Removal of chromium (VI) from electroplating industry wastewater using bagasse fly ash —a sugar industry waste material. Environmentalist 19:129–136

Gupta VK, Gupta M, Sharma S (2001) Process development for the removal of lead and chromium from aqueous solutions using red mud—an aluminum industry waste. Water Res 35:1125–1134

Gupta VK, Mohan D, Sharma S (2003a) Removal of lead from wastewater using bagasse fly ash—a sugar industry waste material. Sep Sci Technol 33:1331–1343

Gupta VK, Jain CK, Ali I, Sharma M, Saini VK (2003b) Removal of cadmium and nickel from wastewater using bagasse fly ash—a sugar industry waste. Water Res 37:4038–4044

Gupta VK, Mittal A, Gajbe V, Mittal J (2006a) Removal and recovery of the hazardous azo dye Acid Orange 7 through adsorption over waste materials: bottom ash and de-oiled soya. Ind Eng Chem Res 45:1446–1453

Gupta VK, Mittal A, Kurup L, Mittal J (2006b) Adsorption of a hazardous dye—erythrosine over hen feathers. J Colloid Interface Sci 304:52–57

Gupta VK, Jain R, Mittal A, Mathur M, Shalini S (2007a) Photochemical degradation of the hazardous dye Safranin-T using TiO2 catalyst. J Colloid Interface Sci 309:464–469

Gupta VK, Jain R, Varshney S (2007b) Removal of Reactofix golden yellow 3RFN from aqueous solution using wheat husk- an agricultural waste. J Hazard Mater 142:443–448

Ho YS, McKay G (1998) Sorption of dye from aqueous solution by peat. J Chem Eng 70:115–124

Kurniawan TM, Chan GYS, Lo WH, Babel S (2006) Physico-chemical treatment techniques of wastewater laden with heavy metals. Chem Eng J 118:83–98

Langmuir I (1918) Adsorption of gases on plain surfaces of glass mica platinum. J Am Chem Soc 40:1316–1403

Mckay G, Blair HS, Gardener JR (1982) Adsorption of dyes on Chitin I. Equilibrium studies. J Appl Poly Sci 27:3043–3057

Mercier L, Pinnavaia TJ (1998) A functionalized porous clays heterostructure for heavy metal ion ($Hg^{2+}$) trapping. Microporous Mesoporous Mater 20:101–106

Mittal A, Jain R, Mittal J, Varshney S, Sirkarwar S (2010) Removal of Yellow ME 7 GL from industrial effluent using electrochemical and sorption technique. Int J Environ Pollusion 43:308–323

Mohan D, Gupta VK, Srivastava SK, Chander S (2001) Kinetics of mercury adsorption from wastewater using activated carbon derived from fertilizer waste. Colloids and Surfaces A 177:169–181

Sharma A, Bhattacharyya KG (2004) Adsorption of chromium(VI) on *Azadirachta indica* (Neem) leaf powder. Adsorption 10:327–338

Srivastava SK, Gupta VK, Mohan D (1996) Kinetic parameters for the removal of lead and chromium from wastewater using activated Carbon developed from fertilizer waste material. Environ Modell Assessment 1:281–290

Srivastava SK, Gupta VK, Mohan D (1997) Removal of lead and chromium by activated slag—a blast-furnace waste. J Envorn Engg 123:461–468

Tchinda AJ, Ngameni E, Walcarius A (2006) Thiol functionalized clay heterostructures (PCHs) deposited as thin films on carbon electrode: towards mercury(II)sensing. Sens Actuator B121:113–123

Tonle IK, Ngameni E, Walcarius A (2004) From clay- to organoclay-film modified electrodes: tuning charge selectivity in ion exchange voltammetry. Electrochim Acta 49:3435–3443

Ullruich SM, Tanton TW, Abdrasthistova SA (2001) Mercury in the aquatic environment: a review of factors affecting methylation. Crit Rev Environ Sci Technol 31:241–293

Vasudevan S, Lakshmi J (2011) Effects of alternating and direct current in electrocoagulation process on the removal of cadmium from water. Sep Purifi Technol 80:643–651

Vasudevan S, Sozhan G, Ravichandran S, Jayaraj J, Lakshmi J, Margrat Sheela S (2008) Studies on the removal of phosphate from drinking water by electrocoagulation process. Ind Eng Chem Res 47:2018–2023

Vasudevan S, Lakshmi J, Sozhan G (2009) Studies on the removal of iron from drinking water by Electrocoagulation— a Clean Process. Clean 37:45–51

Vasudevan S, Lakshmi J, Vanathi R (2010) Electrochemical coagulation for chromium removal: Process optimization, Kinetics, Isotherm and Sludge characterization. Clean 38:9–16

Veli S, Ozturk T (2005) Kinetic modelling of adsorption of reactive azo dye on powdered activated carbon and pumice. Fresenius Environ Bull 14:347–353

Walcarius A, Etienne M, Sayen S, Lebeau B (2003) Grafted silicas in electroanalysis amorphous versus ordered mesoporous materials. Electroanalysis 15:414–421

WHO Guidelines for drinking water quality (1993) Geneva: World Health Organization. Vol. 1–3:45

Zhu X, Alexandratos SD (2006) Determination of trace levels of mercury in aqueous solutions by inductively coupled plasma atomic emission spectrometry: elimination of the memory effect. Microchem J 81:37–41